Indian Journal of Pure & Applied Physics
Vol. 57, November 2019, pp. 793-802

Electronic, mechanical, thermodynamic and optical properties of CdS under pressure

P K Saini[a,b*], D S Ahlawat[b], S Daoud[c] & D Singh[d]

[a]Department of Physics, Government College, Hansi 125 033, India
[b]Department of Physics, Chaudhary Devi Lal University, Sirsa 125 055, India
[c]Laboratoire Matériaux et Systèmes Electroniques (LMSE),
Université Mohamed Elbachir El Ibrahimi de Bordj Bou Arreridj, Bordj Bou Arreridj 34000, Algérie
[d]M M University, Ambala 133 207, India

Received 31 May 2018; accepted 6 July 2019

We report high pressure study of CdS using the full-potential linear augmented plane wave (FP-LAPW) method based on density functional theory approach. In this approach, generalized gradient approximation (GGA) and Engel- Vosko generalized gradient approximation (EV-GGA) have been used for the exchange correlation potential in the calculations. The equilibrium lattice constant, electronic band structure, elastic constants, Debye temperature and melting temperature of binary solid CdS have been calculated under ambient and high pressure. Furthermore, the linear optical properties such as dielectric function, absorption, optical conductivity reflectivity, refractive index and energy loss are computed and analyzed in detail within the energy range up to 14 eV. The obtained results are in good agreement with earlier reported experimental and other theoretical results.

Keywords: Electronic band structure, Elastic constant, Debye temperature, Optical constants, WIEN2k

1 Introduction

The IIB-VIA semiconductor, cadmium sulfide has gained wide attention because of its outstanding electronic, optical properties and technological importance[1-7]. The CdS is very important semiconductor which is widely used in different fields as it has many applications in photodetectors, solar cell, forming quantum dots and passivating the surfaces of other materials. The CdS exists in hexagonal wurtzite structure (WZ)) or cubic zincblende structure (ZB). It is a direct band gap semiconductor. Due to the thermal stability and color in yellow of CdS can form pigments in colors ranging from deep red to yellow with the addition of CdTe[8]. The electronic properties of CdS have been of considerable investigation by both theories and experiments. The band gap is very important parameter which can affect significantly device transport properties. Xu and Ching[1] have observed the energy gap of 2.02 eV using the first-principles orthogonalized linear combination of atomic orbital method, which is in reasonable agreement with experimental values[9,10]. Zakharov *et al*. calculated quasi-particle band structures of CdS using the GW approximation and obtained satisfactory agreement of results when compared with the experiment[2]. Further, Wei *et al*. explained the structure stability of CdS in both zinc-blende and wurtzite structures using the band structure calculations[3]. The investigations of phase transitions also have been extensively studied by experimentally and theoretically using different methods[11-15].

However, most of the above mentioned studies were carried out experimentally and there were comparatively smaller effort to understand the theoretical electronic, elastic, thermodynamic and optical properties which are important for better understanding for this class of materials at high pressure.

The present study provides the significant properties of CdS binary compound at different pressure and different phases. In this work, we have used WIEN2k code for investigation of volume collapse, band gap, elastic constants, average sound velocities, Debye temperature, melting temperature and optical properties of CdS semiconductor compound at ambient zinc-blende (B3) and high pressure rocksalt (B1) phases. The first principles calculations are one of the most powerful tool for theoretical studies of various properties of the condense matter with great accuracy.

*Corresponding author (E-mail: pawansaini2005@gmail.com)

2 Method of Computations

The calculations have been carried out with a self-consistent scheme by solving the Kohn-Sham equations, using a FP-LAPW method in the framework of the density functional theory (DFT) as implemented in the WIEN2K code[16]. The generalized gradient approximation (GGA) was used for the exchange-correlation potential[17-22]. In the method, the unit cell was divided into two regions. The spherical harmonic expansion was used inside the non-overlapping spheres of muffin-tin radius (Rmt) and the plane wave basis set in the interstitial region (IR) of the unit cell. The Rmt for Cd and S were chosen in such a way that the spheres did not overlap. For expansion of the basis function, we set $R_{mt}K_{max}$=8, which controlled the size of the basis set, where K_{max} is the plane wave cut-off and R_{mt} is the smallest muffin-tin radius of atomic sphere radii. The maximum value of l were taken as l_{max}=10, while the charge density is Fourier expanded up to G_{max}=14. For the calculation of electronic properties calculation we have used 72 k-points in the irreducible Brillouin zone for structural optimization. A denser sampling of the BZ was used to calculate the optical properties of the sample. A mesh of 3000 k-points was used for the optical calculations. Accurate convergence criteria have been considered for calculation of all parameters.

3 Results and Discussion

3.1 Electronic properties

The calculated total energies are fitted to the Murnaghan's equation of state (EOS)[23] to obtain the pressure-volume relationship (P=dE/dV) for the both zinc-blende (B3) and rock-salt (B1) phases. The position of minimum of EOS defines the equilibrium lattice parameter and unit cell volume at ambient and high pressure. The equilibrium lattice constants are obtained by calculating total energies by changing the volume. The optimized lattice constant of CdS is obtained as 5.89 Å in zinc blende phase whereas 5.48 Å for rock salt phase under the application of high pressure at about 3.85 GPa. The stability of particular structure corresponds to the lowest Gibbs free energy[31], which is given by:

$$G = U + PV - TS \quad \ldots (1)$$

Where, *U* is the internal energy, *P* the pressure, *V* the volume, *T* the temperature and *S* is the entropy.

We have optimized (at T=0 K) both the cell parameters and atomic positions for zinc-blende (B3) and NaCl (B1) phases to investigate the pressure-induced structural transition. At T=0 K, the Gibbs free energy can be taken equal to the enthalpy[31]:

$$H = U + PV \quad \ldots (2)$$

The calculated enthalpies vs pressure plots for both phases are displayed in Fig. 1. The enthalpies versus pressure curves corresponding to the B3 and B1 phases suggesting that the transition pressure (Pt) from B3 to B1 is 3.85 GPa. The obtained value of phase transition pressure is well agreed with the literature[34]. The equation of state curves (plotted between V (p)/V (0) and pressure) for both zinc-blende and rock-salt phases are plotted in Fig. 2. From these curves, one can estimate the volume collapse in the point of transition (3.85 GPa). The computed value of the volume collapse is estimated at about 18 %.

It is clearly seen that the equilibrium atomic cell volume reduces on the application of high pressure, which corresponds to the change in the lattice parameter and density. The obtained lattice constants are 5.89 and 5.48 angstrom for B3 and B1 phases,

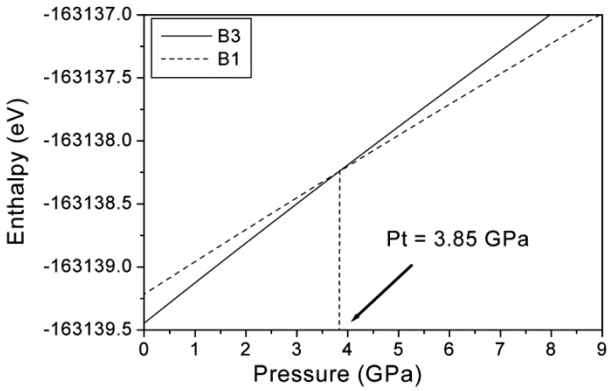

Fig. 1 – Enthalpy vs pressure of CdS.

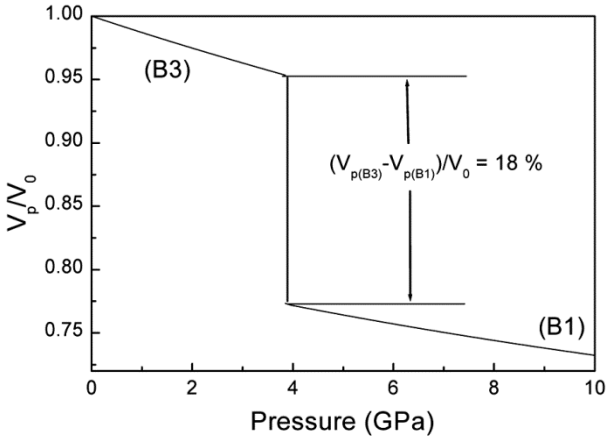

Fig. 2 – Volume vs pressure of CdS.

respectively in good agreement with the literature[13,24-26]. Figure 3 represents the change in density with pressure of CdS. The obtained values of density are 4.658 and 5.791 g (g/cm^3) for ambient phase (B3) and high pressure (B1) phase, respectively. It should be noted that at high pressure the density of CdS is found to be increased as compared to ambient pressure. Because the lattice distance of atoms decreased and come closer under pressure.

By using optimized structural results, the electronic structures including the band structure, DOS, and PDOS are computed for Zinc-blende and rock-salt phase of CdS. It is well known fact that DFT underestimates the energy gaps up to 40% when compared with the experimental value. This may be due to the reason that the exchange correlation term cannot be calculated accurately. However, EV-GGA improves the band gap in contrast to the local density approximation (LDA) and generalized gradient approximation (GGA). Therefore, we have used EV-GGA instead of LDA and GGA[36]. Figure 4 and 5 represents the calculated band structure of CdS in ZB and RS phase. The calculated direct band gap 1.62 eV along the Γ direction listed in Table 1 and found well agreement with the experimental value. Further, it was found that the direct band gap increases with the pressure. It may be due to the reason that when a hydrostatic pressure is applied to a direct-band gap semiconductor, the inter-atomic distance decreases, and the direct band gap increases while the indirect band gap decreases.

A very small indirect band gap about 0.1 eV is seen in L-X direction, indicating a semi metallic nature of

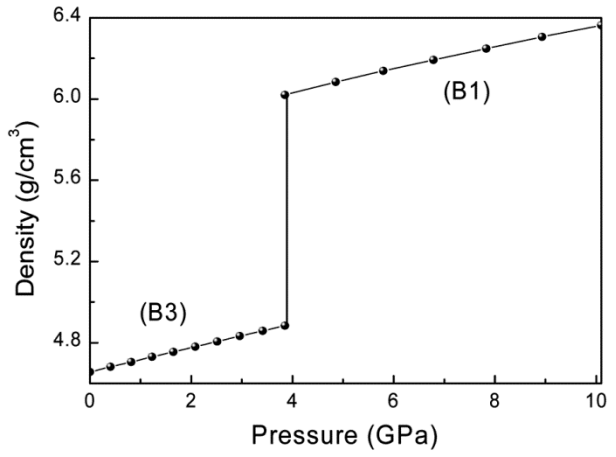

Fig. 3 – Density vs pressure of CdS

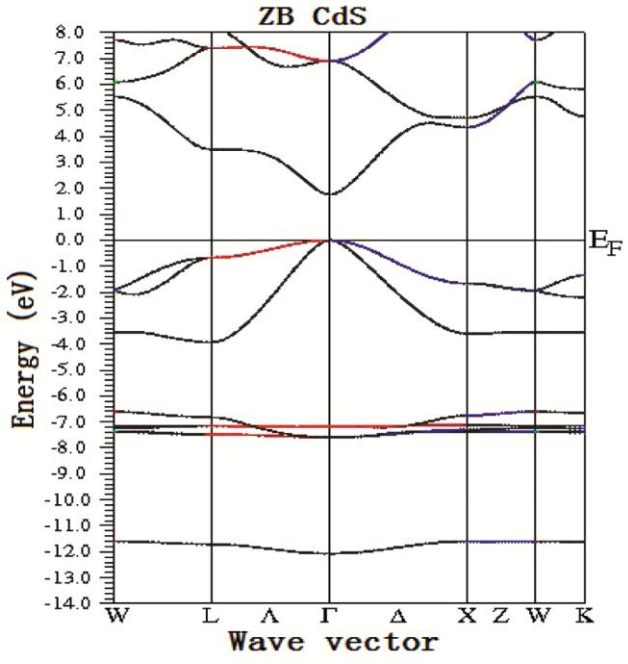

Fig. 4 – Band structure in ZB phase of CdS.

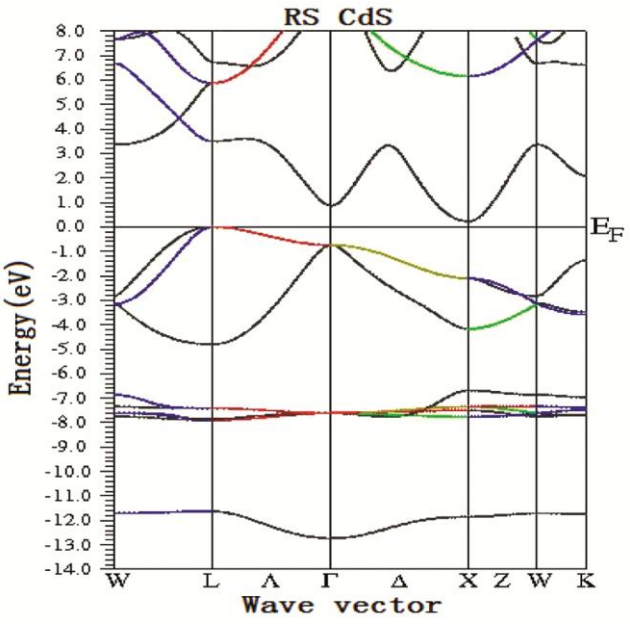

Fig. 5 – Band structure in RS phase of CdS.

Table 1 – The calculated direct-band gaps for zinc blende phase of CdS using EV-GGA with the other theoretical and experimental work

Calculations	Direct band gap (eV) at Γ point
Present	1.62
Theory (Ref. [2])	1.37
Theory (Ref. [27])	2.61
Theory (Ref. [25])	1.45
Experimental (Ref. [26])	2.55

cadmium sulphide in RS phase. Fermi energy is shown by dotted line. In order to indicate the overall profile of the different bands of CdS, we have identified the bands with their corresponding electronic states. It can be seen that the lowest-lying band in the valence band region (appears between 10.3 eV-11.6 eV) mainly arises from the 3s states of S while the bands in valence region just below E_F are predominantly due to 5s and 5p orbital of Cd. The conduction band above E_F is mainly due to 4d states of Cd which hybridize with p and d states of S. Further, we have calculated and plotted the total density of states (TDOS) and partial density of (PDOS) for ZB and RS phases of CdS as shown in Figs 6 and 7. The electronic state consisting of three regions: lower valence band (LVB), upper valence band (UVB) and conduction band (CB). The total density of state (DOS) describes the electron distribution in the energy spectrum. It may be seen from the different partial DOS histograms that the peaks found in lowest energy region mainly arise from the s states of S while the peaks in next higher energy region just below E_F are predominantly due to 5s and 5p orbital of Cd. The peaks obtained in the next further

Higher region (in the conduction band above E_F) are mainly due to 4d states of Cd which hybridize with p and d states of S. The LVB density of the state peak is found at -12 eV and it has a 4.2 eV width which is separated by a large gap of about 8.2 eV from the UVB states existing at about 4 eV. There is no sharp peak found near the Fermi level for s-3p while a narrow sharp peak found in the UVB near -4 eV. This means that the partial DOS for each atom are not equal. Finally, Fermi energy is calculated and plotted in all above figures by dotted line. Further, it is observed that the Fermi level is found to be shifting

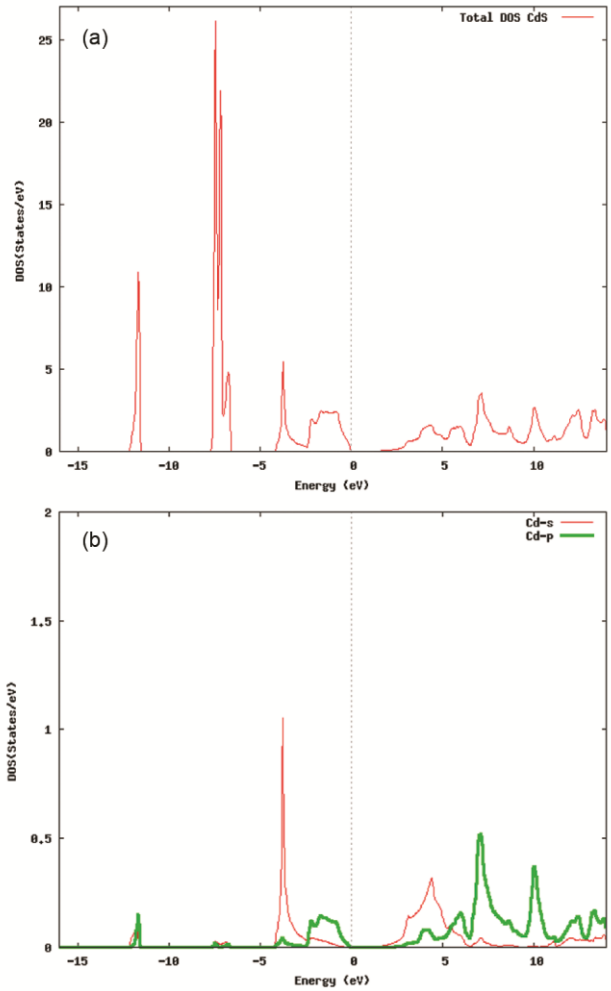

Fig. 6 – (a) Total DOS and (b) Cd-s partial DOS of CdS in ZB phase.

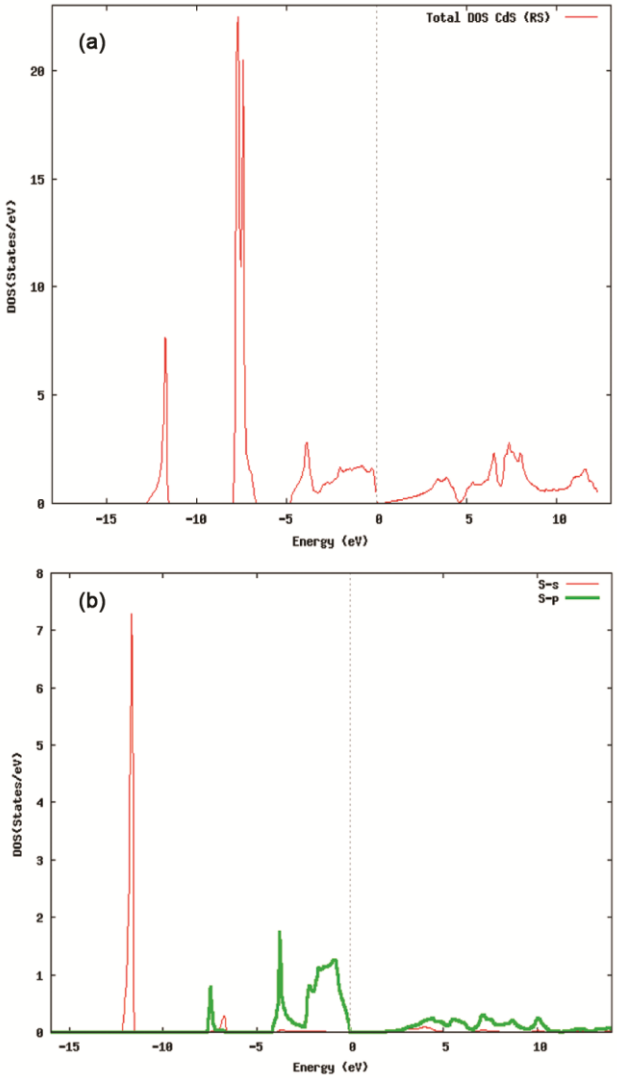

Fig. 7 – (a) Total DOS and (b) S-s partial DOS of CdS in RS phase.

gradually to higher energies with increase in pressure. It may be due to increase in electron concentration under pressure. Due to change in the Fermi energy, conduction band width (which is the difference in energy between Fermi level and lowest eigen value corresponding to G-point) is found to become broader with increase in pressure.

3.2 Elastic properties

The mechanical and dynamical behaviors of crystals are linked with the elastic constants and provide significant information about the nature of forces existing in the solids. We have used the charpin method within Wien2k code to compute the elastic constants of cubic CdS in both phases. A small strain must be applied to the crystal to obtain the elastic constants. Further, they can be estimated by computing the total energy as a function of proper lattice deformation. For mechanical stability of cubic crystal, three independent elastic constants C_{11}, C_{12} and C_{44} should match with the conditions[29]: C_{11}-C_{12}>0, C_{44}>0, C_{11}+2C_{12}>0. The calculated elastic constants are also found to obey the cubic stability conditions including the fact that C_{12} should be smaller than C_{11}. The following sets of three equations were used for computing the elastic constants:

$$B = (C_{11} + 2C_{12})/3 \quad \ldots (3)$$

$$\Delta E_{rhomb} = \frac{1}{6}(C_{11} + C_{12} + 4C_{44})V_0\delta^2 \quad \ldots (4)$$

$$\Delta E_{tetra} = 6(C_{11} - C_{12})V_0\delta^2 \quad \ldots (5)$$

The first equation gives the relationship between the bulk modulus and elastic constants whereas, the second equation represents the variation of strain energy with volume conserving rhombohedral strain (δ). The relationship of strain energy with the volume conserving tetragonal strain (δ) is represented by third equation.

In our calculations, we consider only small lattice distortions in order to maintain the elastic domain of the crystal. Furthermore, other elastic constants like shear modulus G, Young modulus E, anisotropic parameter A, Kleinmann parameter ξ and Poisson ratio γ have also been calculated for the ZB and RS structures of CdS and presented with the already reported theoretical calculations in the Table 2. The shear modulus or modulus of rigidity (G) describes an items tendency to shear, i.e., deformation of shape at constant volume when acted upon by divergent forces. Hence, shear modulus (G) can be expressed as:

$$G = \frac{G_V + G_R}{2} \quad \ldots (6)$$

Here, Reuss modulus G_R is given by:

$$G_R = \frac{5(C_{11} - C_{12})C_{44}}{4C_{44} + 3(C_{11} - C_{12})} \quad \ldots (7)$$

The Voigt modulus G_v is defined as:

$$G_V = \frac{1}{5}(3C_{44} + C_{11} - C_{12}) \quad \ldots (8)$$

The Kleinmann parameter is an important parameter relating to the position of the cation and anion sublattices as given by relation[37]:

$$\xi = \frac{C_{11} + 8C_{12}}{7C_{11} + 2C_{12}} \quad \ldots (9)$$

Further, Young's modulus, also known as the tensile modulus or elastic modulus is a measure of the stiffness of an elastic material and also used to characterize the materials. In anisotropic materials, Young's modulus may have different values depending on the direction of the applied external force with respect to the material's structure. If the material is stretched rather than compressed, it usually contract in the directions transverse to the direction of stretching. This is a common observation when a

Table 2 – The calculated elastic constants C_{ij} (GPa), bulk modulus B (GPa), shear modulus G (GPa), Young modulus E (GPa), anisotropic parameter A, Kleinmann parameter ξ and Poisson ratio γ for CdS in the ZB and RS structures

CdS	Calculations	C_{11}	C_{12}	C_{44}	B	G	E	A	ξ	γ
ZB phase	Present work	90.26	44.19	39.27	59.55	31.70	80.76	0.358	0.61	0.273
	Theory ([Ref. 29])	81.79	61.06	31.0						
	Theory (Ref.[35])	89.38	53.52	39.11						
	Theory (Ref. [25])	97.8	59.7	30.6						
	Exp.									
RS phase	Present work	121.83	53.12	44.91	76.03	40.33	102.8	0.173	-	0.274
	Theory (Ref.29)	157.82	59.66	35.33						

rubber band is stretched, when it becomes markedly thinner. The Poisson ratio is the ratio of relative contraction to relative stretching of material. In certain rare cases, a material may actually shrink in the transverse direction when compressed (or expand when stretched) which will produce a negative value of the Poisson ratio. Thus, the Young modulus E and the Poisson ratio γ are connected to the hardness for polycrystalline materials. These quantities can be expressed by the following relations[37]:

$$E = \frac{9BG}{3B+G} \quad \ldots (10)$$

$$\gamma = \frac{1}{2}\left(\frac{3B-E}{3B}\right) \quad \ldots (11)$$

The Poisson's ratio of a stable, isotropic and linear elastic material cannot be less than −1.0 or greater than 0.5 due to the constraint that Young's modulus, the shear modulus and bulk modulus have its positive values.

The width of the bonds of shear modulus is related to the anisotropy constants as given by the relation:

$$A = \frac{2C_{44}+C_{12}-C_{11}}{C_{11}} \quad \ldots (12)$$

As the anisotropy constant tends to approaches to unity, the gap between the bonds disappear and the crystal goes to isotropic phase. It is clearly observed that CdS under high pressure also possesses mechanical stability. The elastic constants are strongly affected by applied pressure. It can be noted that the elastic constants C_{11}, C_{12} and C_{44} are increased with the pressure increased because the lattice parameter of CdS becomes shorter under high pressure. The ductility of CdS is given by an important parameter B/G ratio. It is found 1.87 for ZB phase and 1.90 for RS phase. It should be noted that at high pressure CdS is found more ductile than ambient phase. The calculated values of elastic constants are found in reasonable agreement with the available theoretical and experimental results in the literature for ZB phase. The calculated results are obtained in good agreement with the earlier reported theoretical results [29] for high pressure RS phase. Whereas, to the best of our knowledge, there is no experimental data of elastic parameters available for high pressure RS phase of CdS in the literature and so comparison could not be possible.

3.3 Thermodynamic properties

In this section we have calculated the average sound velocity, Debye temperature, melting temperature and Vickers hardness for both ZB and RS phase of CdS. The observed results are shown in Table 3. Debye temperature is important fundamental parameter related to the many physical properties of solids like elastic constant, specific heat and melting temperature. Debye temperature calculated from elastic constants at low temperature is same as determined from specific heat measurement. Debye temperature can be obtained by using the average sound velocity (Vm), which strongly depends upon the directions in an anisotropic material. The two type of waves, longitudinal and shear waves are observed in solids. Using the stiffness constant C_{ij} and crystal density of CdS, we have calculated the bulk sound velocity. The average sound velocity is given by the following formula[31]:

$$v_m = (2/v_t^3 + 1/v_l^3)/3)^{-1/3} \quad \ldots (13)$$

Where, v_t and v_l are the transverse and longitudinal sound velocity obtained by using the isotropic shear modulus G, the bulk modulus B and the crystal density g, they are calculated by using the following formulas[31]:

$$v_l = \sqrt{(3B+4G)/3\rho}\text{, and } v_t = \sqrt{G/\rho} \quad \ldots (14)$$

The Debye temperature (θ_D) can be calculated from the average sound velocity v_m by using the following formula[31]:

$$\theta D = (h/k_B)(3/4\pi V_\alpha)^{1/3} v_m \quad \ldots (15)$$

Where, h is the Planck constant, k_B is the Boltzmann constant and V_a the atomic volume.

Another empirical formula was usually also used to predict the Debye temperature Θ_D of materials from

Table 3 – Calculated value of density, longitudinal sound velocity, transverse sound velocity, average sound velocity, Debye temperature, melting temperature and Vickers hardness for both ZB and RS phases of CdS

Parameters	ZB phase		RS phase	
CdS	This work	Others	This work	Others
G(g/cm^3)	4.658		5.791	
v_l(m/s)	4675.4		4734.6	
v_t(m/s)	2608.9		2639.4	
v_m(m/s)	2904.7		2938.8	
θ_D(K)	293[a], 299[b]	265[c] 286[d]	319[a], 324[b]	
T_m(K)	1086		1273	
H_v(GPa)	4.22	3.2[e]	5.29	

[a]equation (15), [b]equation(16), [c]Ref.38, [d]Ref.39, [e]Ref.40

their elastic constant C_{ij}. This formula was applied successfully by Siethoff[32]. The Debye temperature Θ_D is given as function of the elastic constant C_{ij} by the following expression[32]:

$$\theta_D = C_S s^{-1/6}\left(aGc/M\right)^{1/2} \quad \ldots (16)$$

Here, Cs is a further constant and s is the number of atoms in the crystallographic unit cell. The elastic constants enter Eq. (16) via the elastic modulus[32] G, which may be written as:

$$Gc = \left[C_{44}\left[C_{44}\left(C_{11}-C_{12}\right)/2\right]^{1/2}\left(C_{11}-C_{12}+C_{44}\right)/3\right]^{1/3} \quad \ldots (17)$$

The melting temperature[31] (T_m):

$$T_m = 553 + 5.91\ C_{11}$$

The Vickers hardness (Hv) can be expressed by several formulas[33], among them the following:

$$H_v = 2\left(G^3/B^2\right)^{0.585} - 3 \quad \ldots (18)$$

Where, G is the isotropic shear modulus and B is the Bulk modulus.

The calculated average sound velocity, Debye temperature, melting temperature (Tv), Vickers hardness (Hv) of CdS are found to be increased in high pressure RS phase than ZB phase. Debye temperature calculated from average sound velocity (using Eq. 15) is found very close to the elastic constant empirical formula (using Eq. 16). Unfortunately, there is no experimental and theoretical data available in the literature for RS phase of CdS and so comparison could not be possible.

3.4 Optical properties

The frequency dependent dielectric function has been used to describe the linear optical properties. The optical properties are obtained from the complex dielectric-function spectrum $\varepsilon_{\alpha\beta}(\omega)$ = Re $\varepsilon_{\alpha\beta}(\omega)$ + i Im $\varepsilon_{\alpha\beta}(\omega) = \varepsilon_1(\omega) + i\varepsilon_2(\omega)$. The imaginary part of the dielectric tensor can be computed from the electronic band structure of solid. The dielectric function, $\varepsilon_2(\omega)$ is strongly correlated to the joint density of states (DOS) and transition momentum matrix elements. Using the dispersion of real and imaginary parts of dielectric functions one can calculate dispersion of other optical parameters such as refractive indices, optical conductivities, absorption coefficient, extinction coefficient and e loss function. We have used the following well- known relations[28] for the calculation of optical properties:

$$\text{Im}\ \varepsilon_{\alpha\beta}(\omega) = \frac{4\pi e^2}{m^2\omega^2}\sum_{c,v}\int_0^\infty dk\langle c_k \mid P^\alpha \mid v_k\rangle\langle v_k \mid P^\beta \mid c_k\rangle\left(\varepsilon_{ck}-\varepsilon_{vk}-\omega\right) \quad \ldots (19)$$

$$\text{Re}\ \varepsilon_{\alpha\beta}(\omega) = +\frac{2}{\pi}P\int_0^\infty \frac{\omega'\text{Im}\varepsilon_{\alpha\beta}(\omega')}{\omega'^2-\omega^2}d\omega' \quad \ldots (20)$$

The optical conductivity is given by:

$$\text{Re}\ \sigma_{\alpha\beta}(\omega) = \frac{\omega}{4\pi}\text{Im}\ \varepsilon_{\alpha\beta}(\omega) \quad \ldots (21)$$

The refractive index, n (ω) is given by:

$$n(\omega) = \sqrt{\frac{|\varepsilon(\omega)| + \text{Re}\varepsilon(\omega)}{2}} \quad \ldots (22)$$

The extinction coefficient, k (ω) is given by:

$$k(\omega) = \sqrt{\frac{|\varepsilon(\omega)| - \text{Re}\varepsilon(\omega)}{2}} \quad \ldots (23)$$

The linear optical properties of cubic CdS in ZB and RS phase has been investigated by calculating the optical parameters, dielectric function $\varepsilon(\omega)$, refractive index n(ω) and eloss function L(ω). The dispersion of the real and imaginary parts of dielectric function, $\varepsilon_2(\omega)$ and $\varepsilon_1(\omega)$, for CdS in ZB and RS phase are

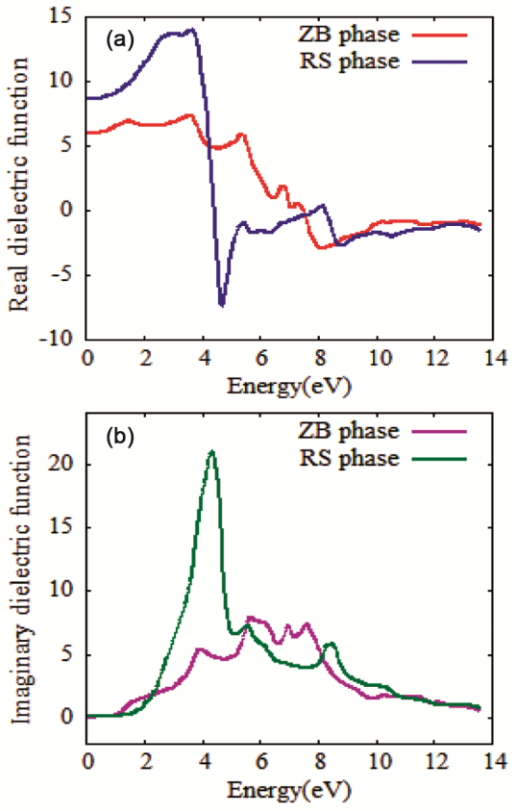

Fig. 8 – (a-b) Real and imaginary dielectric function in ZB and RS phases of CdS.

shown in the Fig. 8(a and b).

Figure 8(a) shows that the first main and highest peak value of ε_1 (ω) exists at energy 3.51 eV for ZBb while 3.52 eV for RS phase, respectively. The static dielectric constant ε_1 (0) without any contribution from lattice vibration is equal to about 5.97 for ZB Cd while 8.63 for RS CdS, respectively. It may be underline that wide band energy gap yields a smaller value of ε_1 (0). The analysis of ε_2 (ω) spectra of Fig. 8(b) shows the threshold energy occurring at 0.53 eV and 1.2 eV for CdS in ZB and RS phase. It is clear from the spectrum that the major energy spectral peaks for ZB phase situated at 5.67 eV for CdS, as well as for the RS phase 4.20 eV for CdS, respectively. The highest peak in ε_2(ω) corresponds to the transition from occupied Cd-s to unoccupied S-s band states.

Figure 9(a) shows the theoretically obtained absorption spectrum α(ω) for the CdS compound in ZB phase. It is noted that the absorption edge start from about 0.16 eV corresponding to the direct Γ- Γ transition. The absorption spectrum α(ω), shows a very intense absorption, which occurs at about 8 eV for CdS due to excitations of photons. The find out results are seems to be similar to the experimental findings reported earlier[41] with reference to the peaks position and height. In case of RS phase the absorption edge start from about 0.20 eV for CdS, corresponding to the transition of electrons from valence band to conduction band. The optical conductivity spectra are obtained for ZB and RS phases as shown in Fig. 9(b), respectively. The inter-band transition is called Drude transition and photon absorption by electron is called inter-band absorption. As shown in the Fig. 9(b), the optical conduction starts from the energy of about 0.10 eV for CdS in the ZB phase and by increasing photon energy, the optical conduction arises and reached at the maxima. The reason of starting optical conduction σ (ω), from above said energy range, is the gap of energy. As the excited electrons have no enough energy to pass the energy gap, and transfer to the conduction band. It is observed that all the peak structures in σ (ω) are shifted a little towards the higher energies with decrease in the peak heights as compared to their corresponding peaks in RS spectrum. The results obtained are found similar to the experimental findings[41] reported by others with reference to the peaks position and height. The optical conduction σ(ω) starts with energy of about 0.16 eV for CdS in

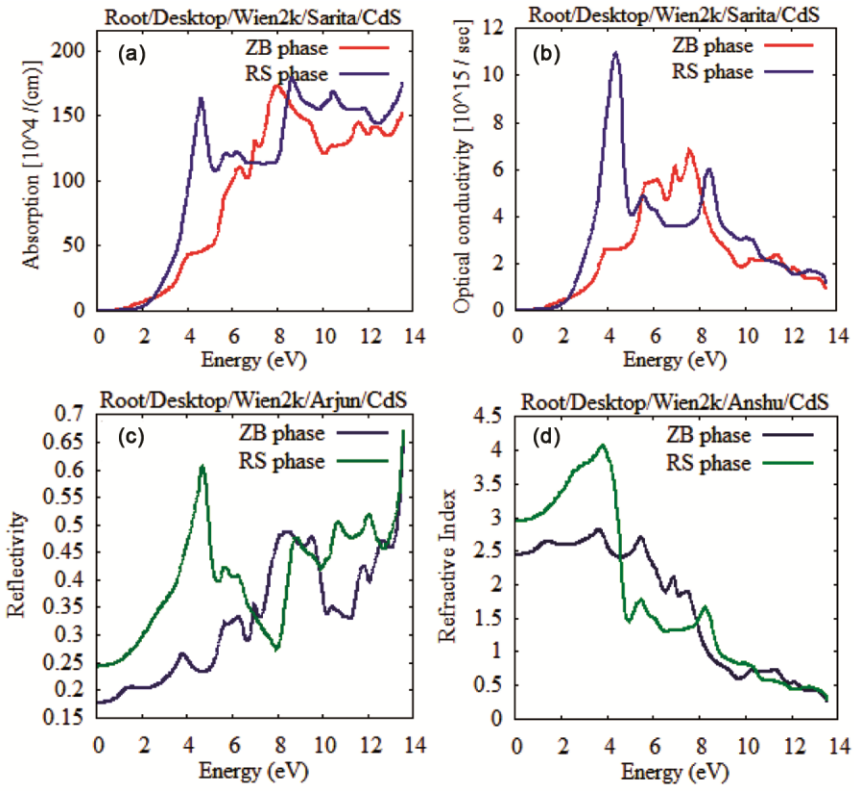

Fig. 9 – (a-d) Absorption, optical conductivity, reflectivity and refractive index in ZB and RS phases of CdS.

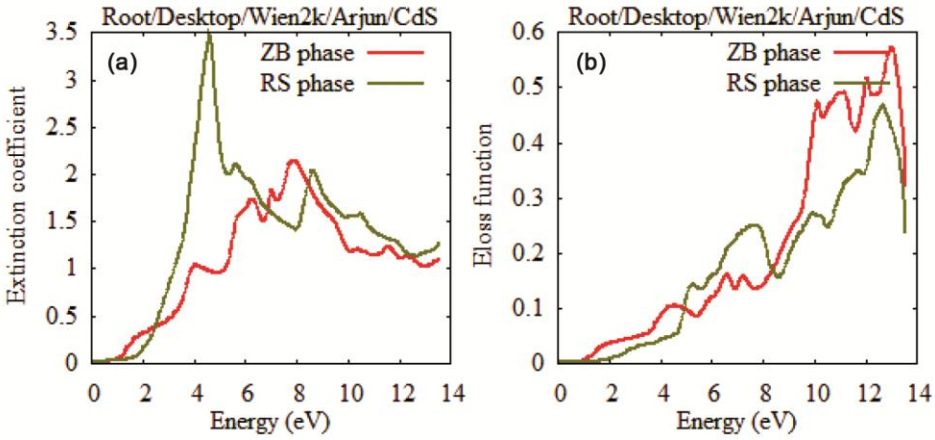

Fig. 10 – (a-b) Extinction coefficient and Eloss function in ZB and RS phases of CdS.

the RS phase and by increasing photon energy, the optical conduction rises and reached at maximum similar to the case of ZB phase. It is observed that all the structures in σ (ω), are shifted a little towards the lower energies with increase in the peak heights as compared to ZB case.

Figure 9(c), show the calculated frequency dependent reflectivity spectra R (ω) for the CdS compound in ZB and RS phases. A similar reflection spectrum is found when compared with the reported experimental data[41] with reference to the peaks position and height. Thus, the reflectivity spectrum of the investigated compound CdS shows some difference with very similar features and agreed well with one another for ZB and RS phases. This is due to the fact that the band structures for this compound are indeed seem to be quite similar and a small difference of band structure is responsible for the difference in reflectivity spectra of ZB and RS phases. A strong reflectivity maximum is observed in the between energy range 6.5 eV-10.2 eV which arises as a result of inter-band transitions. Whereas, in RS phase a strong reflectivity minimum is also observed at energies ranging from about 2.5-4 eV this is representing a collective plasma resonance. Whereas, in RS phase the strong reflectivity maximum between energy ranges between 4.5-9.25 eV arises from the inter-band transitions. The depth of the plasma minimum can be determined by the imaginary part of the dielectric function at the plasma resonance and is representative of the degree of overlap between the inter-band absorption regions. Figure 9(d) represents the refractive index spectra for the CdS compound in ZB and RS phases. This shows that the refractive index is significant only up to of 3.85 eV for ZB and beyond this energy it starts to drop and after 5.5 eV it drops sharply. In RS phase the refractive index is significant only up to 4.28 for CdS and beyond this energy it drops sharply. Our theoretically calculated static refractive index is 2.46 and 2.99 for ZB and RS phases, respectively. There is no theoretical or experimental data available in literature to compare the results.

The extinction coefficient k (ω) which is calculated and presented in Fig. 10(a) for ZB and RS phase. The local maxima of the extinction coefficient k (ω) for ZB and RS phases found correspond to the zero of ε_1 (ω) at (6.50 eV) and 4.25 eV refer to Fig. 8(a) for ZB and RS phase, respectively. The electron energy loss function L(ω), is a significant factor and found related to the energy loss of fast electrons traversing in the material. The electrons, which excite the atomic electrons of the outer shell is called valence loss or valence inter-band transitions. In the case of inter-band transitions, which consist mostly of plasmon excitations, the scattering probability for volume losses is directly connected to the energy loss function. In the Fig. 10(b), the most prominent peak in the energy loss spectrum is associated with the plasmon peak and located at 12.93 eV and 12.90 eV for ZB and RS phase, respectively and the corresponding frequency is called plasma frequency[42] ($\hbar\omega_p$). The calculated results are found similar to the experimental findings[43] with regard to the peaks position and height for ZB structure. There is no experimental data available for RS phase in the literature, so comparison could not be possible.

4 Conclusions

In summary, a first principles study has been performed to calculate the various properties of CdS at

ambient and high pressure phases using the FP-LAPW method with the generalized gradient approximation (GGA). The electronic band structure and density of states reveal the existence of band gap 1.62 eV at Fermi level. The structural and elastic parameters have been computed and they are found to be in good agreement with the other available results. Moreover, the Debye temperature, melting temperature and Vickers hardness are also computed and analysed of both phases. Furthermore, the optical parameters such as dielectric function $\varepsilon(\omega)$, refractive index $n(\omega)$ and optical conductivity $\sigma(\omega)$, absorption $I(\omega)$, reflectivity $R(\omega)$ extinction coefficient $k(\omega)$ and eloss function $L(\omega)$ were also be calculated and analyzed. The calculations show a static refractive index of 2.46 and 2.99 for ZB and RS phases of CdS. But, there is no experimental and theoretical data available for RS phase in the literature, so comparisons could not be possible. This high pressure behavior of CdS will further lead to guide more advance experimental and theoretical study of the material and helps the design of devices which can operate under high pressure conditions.

References

1 Xu Y N & Ching W Y, *Phys Rev B*, 48 (1993) 4335.
2 Zakharov O, Rubio A, Blase X, Cohen M L & Louie S G, *Phys Rev B*, 50 (1994) 10780.
3 Wei S & Zhang S B, *Phys Rev B*, 62 (2000) 6944.
4 Tomasulo A & Ramakrishna M V, *J Chem Phys*, 105 (1996) 3612.
5 Kim Y D, Klein M V, Ren S F, Chen Y C, Lou H, Samarth N & Furdyna J K , *Phys Rev B*, 49 (1994) 7262.
6 Fernee M, Watt A, Warner J, Cooper S, Heckenberg N & Rubinsztein-Dunlop H, *Nanotechnology*, 14 (2003) 991.
7 Patidar D, Sharma R, Jain N, Sharma T P & Saxena N S, *Bull Mater Sci*, 29 (2006) 21.
8 Greenwood N N & Earnshaw A, Chemistry of the Elements (Butterworth–Heinemann: Oxford) 2nd Edn (1997).
9 Ley L, Pollak R A, Mcfeely F R, Kowalczyk S P & Shirley D A, *Phys Rev B*, 9 (1974) 600.
10 Weber M J, Handbook of Laser Science and Technology (Cleveland) Vol. III CRC (1986).
11 Edwards A L & Drickamer H G, *Phys Rev*, 122 (1961) 1149.
12 Corll J A, *J Appl Phys*, 35 (1964) 3032.
13 Knudson M D, Gupta Y M & Kunz A B, *Phys Rev B*, 59 (1999) 11704.
14 Zhao X S, Schroeder J, Bilodeau T G & Hwa L G, *Phys Rev B*, 40 (1989) 1257.
15 Venkateswaran U & Chandrasekhar M, *Phys Rev B*, 31 (1985) 1219.
16 Blaha P, Schwarz K, Medsen G K H, Kvasnicka D & Luitz J, WIEN2k An Augmented Plane Wave Plus Local Orbitals Program for Calculating Crystal Properties, Vienna University of Technology ,Vienna, Austria, 2001.
17 Perdew J P, Chevary J A, Vosko S H, Jackson K A, Pederson M R, Singh D J & Fiolhais C, *Phys Rev B*, 46 **(**1992) 6671.
18 Peterson M, Wanger F, Hufnagel L, Scheffler M, Blaha P & Schwarz K, *Comput Phys Commun*, 126 (2000) 294.
19 Schwarz K, *J Solid State Chem*, 176 (2003) 319.
20 Schwarz K & Blaha P, *Comput Mat Sci*, 28 (2003) 259.
21 Schwarz K, Blaha P & Madsen G K H, *Comput Phys Commun*, 147 (2002) 71.
22 Saini P K, Singh D & Ahlawat D S, *Indian J Pure Appl Phys*, 55 (2017) 649.
23 Murnaghan F D, *Proc Natl Acad Sci USA*, 30 (1994) 5390.
24 Benkhettou N, Rached D, Soudini B & Driz M, *Phys State Solids*, 241 (2004) 101.
25 Deligoz E, Colakoglu K & Ciftci Y, *Physica B*, 373 (2006) 124.
26 Madelung O, Schulz M & Weiss H, 17th Edn, Landolt-Borstein: Numerical data and functional relationships in science and technology, (Springer: Berlin) 1982.
27 Duan Y & Jungen M, *Eur Phys J*, 2 (1998) 183.
28 Wooten F, Optical properties of solids, (Academic Press: New York) 1972.
29 Tan J J , Li Y & Ji G F, *Acta Phys Pol A*, 120 (2011) 501.
30 Anderson O L, *J Phys Chem Solids*, 24 (1963) 909.
31 Daoud S, Bioud N & Bouarissa N, *Mater Sci Semicond Process*, 31 (2015) 124.
32 Siethoff H, *Intermetallics*, 5 (1997) 625.
33 Yang R, Zhu C, Wei Q & Zhang D, *Solid State Commun*, 267 (2017) 23.
34 Kheloufi N & Bouzi A, *J Alloys Compd*, 659 (2016) 295.
35 Wright K & Gale J D, *Phys Rev B*, 70 (2004) 035211.
36 Engel E & Vosko S H, *Phys Rev B*, 47(1993) 13164.
37 Harrison W A, Electronic structure and properties of solids (W H Freeman and company :San Francisco) 1980.
38 Nusimovici M A & L J Birman, Proc 7th Int Conf II-VI Semiconducting Compounds, (W A Benjamin Inc: Providence R I USA New York) (1967) 1204.
39 Holland M G, *Phys Rev A*, 134 (1964) 471.
40 Goble R J & Scott S D, *Can Mineral*, 23 (1985) 273.
41 Freeouf J L, *Phys Rev B*, 7 (1973) 3810.
42 Nozieres P, *Phys Rev Lett*, 8 (1959) 1.
43 Adachi S, Optical constants of crystalline and amorphous semiconductors (Springer: New York) 1999.